

Efficiency of the X-mode anomalous absorption in the plasma filament associated with the two upper-hybrid-plasmon decay

A.B. Altukhov², V.I. Arkhipenko¹, A.D. Gurchenko², E.Z. Gusakov², A.Yu. Popov²,

L.V. Simonchik¹, P.V. Tretinnikov², M.S. Usachonak¹

¹ Institute of Physics NAS of Belarus, Minsk, Belarus

² Ioffe Institute, St-Petersburg, Russia

1. Introduction

It was shown firstly at the Textor tokamak [1] that the second harmonic X-mode heating experiments are accompanied by anomalous backscattering phenomena. Theoretical model proposed recently [2] explains the anomalous backscattering as a result of the two upper-hybrid (UH) plasmon parametric decay (TUHPD) instability which has a very low threshold due to nonlinearly excited plasmons trapping in the vicinity of the density maximum that accompanies the magnetic island. The theory [2] also predicts substantial (up to 25%) anomalous absorption due to this process. The aim of this work is to check the efficiency of the X-mode anomalous absorption associated with the TUHPD leading to excitation of the trapped UH waves in the laboratory plasma.

2. Experimental setup

The plasma filament is produced in long glass tube with the inner diameter of 22 mm filled with argon (pressure about 1 Pa) oriented in the direction of the magnetic field (Fig. 1). The magnetic field created by the external electromagnet can be varied from 0 to 45 mT. The glass tube passes through the waveguide (72×34 mm²) in parallel to the wide walls. The RF power of about 100 W at frequency of 27 MHz is supplied to the ring electrodes. The volume averaged

plasma density measured using the cavity diagnostics is about 10^{10} cm⁻³.

The X-mode microwave pulses (up to 210 W) were incident onto the plasma along the waveguide. As the frequency of the launched waves $f_0 = 2.35$ GHz is higher than the upper hybrid (UH) frequency and second harmonic of the electron cyclotron resonance (ECR) frequency, there were no linear mechanisms of the pump absorption, but the collisional one, which is not effective at the experiment conditions.

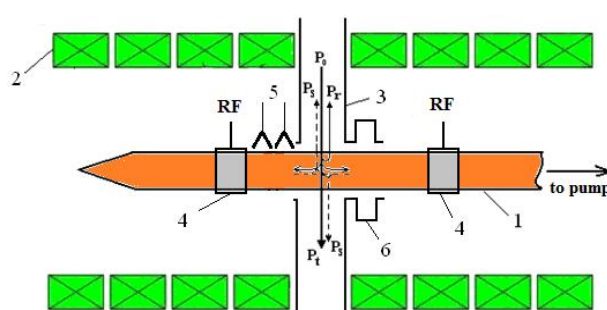


Fig. 1. Schematic of experimental setup. 1 – plasma filament, 2 – magnet coils, 3 – waveguide, 4 – RF electrodes, 5 – antennas and 6 – 10-cm cavity.

effective at the experiment conditions.

3. Theoretical predictions

In this section we adopt the theoretical model developed in [2] for interpretation of the anomalous phenomena observed in the X2 ECRH experiments in the toroidal devices for the case of strongly inhomogeneous collisional plasmas. We analyse the two-plasmon decay excitation in the slab geometry introducing the Cartesian coordinate system with its origin

resting on the filament axis, the coordinate z directed along it and the coordinates x, y imitating the radial and azimuthal coordinates.

The X-mode pump electric field is represented by $\mathbf{E} = \mathbf{e}_y E_0 (P_0, z) \exp(i k_x x - i \omega_0 t)$, where P_0 is

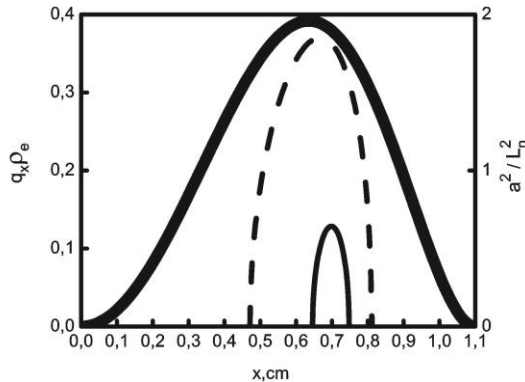


Fig. 2. The dispersion curves of UH waves (left and bottom axes): mode $n = 0$, solid line; mode $n = 4$, dashed line; and $a^2 / L_n^2(x)$ for the parabolic density profile (right and bottom axes) –(thick solid line).

$\phi_2(\mathbf{r}, t) = b_2 \exp(i \omega_0 t / 2)$ is assumed to be much smaller than the density scale length L_n that allows describing them using the following integral equations for their amplitudes

$$\begin{aligned} \int d\mathbf{r}' d\mathbf{q} \exp(i\mathbf{q}(\mathbf{r} - \mathbf{r}')) ((q^2 + \chi_l(\omega_0 / 2, \mathbf{q}, x)) b_1(\mathbf{r}') + \chi_{nl}(\omega_0 / 2, \mathbf{q}, x) b_2(\mathbf{r}')) &= 0, \\ \int d\mathbf{r}' d\mathbf{q} \exp(i\mathbf{q}(\mathbf{r} - \mathbf{r}')) ((q^2 + \chi_l(-\omega_0 / 2, \mathbf{q}, x)) b_2(\mathbf{r}') + \chi_{nl}(-\omega_0 / 2, \mathbf{q}, x) b_1(\mathbf{r}')) &= 0. \end{aligned} \quad (1)$$

In (1) we have introduced the linear electron susceptibility defined with due account of the electron-atomic collisions ν_{ea} and obeying the condition $\chi_l(\omega_0 / 2, \mathbf{q}) = \chi_l(-\omega_0 / 2, \mathbf{q})^*$.

$$\chi_l(\omega_0 / 2, \mathbf{q}) = \frac{2\omega_{pe}^2}{\nu_{te}^2} \left(1 - \sum_{m=-\infty}^{\infty} \frac{\omega_0 / 2 + i\nu_{ea}}{\omega_0 / 2 + i\nu_{ea} - m\omega_{ce}} I_m \left(\frac{q_\perp^2 \rho_e^2}{2} \right) \exp\left(-\frac{q_\perp^2 \rho_e^2}{2}\right) \right), \quad (2)$$

The imaginary part of χ_l describes the collisional damping of UH waves, ρ_e is the electron Larmor radius, ν_{te} is the electron thermal velocity, ω_{pe} and ω_{ce} are the electron Langmuir and cyclotron frequencies, $q_\perp^2 = q_x^2 + q_y^2$. The nonlinear electron susceptibility describing the nonlinear coupling of the daughter UH waves in the presence of the pump E_0 , derived for strongly inhomogeneous magnetized plasmas [3] and obeying the condition $\chi_{nl}(\omega_0 / 2, \mathbf{q}, x) = \chi_{nl}(-\omega_0 / 2, \mathbf{q}, x)^*$ is given by

$$\chi_{nl}(\omega_0 / 2, \mathbf{q}, x) = \frac{8\omega_{pe}^2(x)\omega_{ce}^2}{(\omega_0^2 - \omega_{ce}^2)(\omega_0^2 - 4\omega_{ce}^2)} \left(\frac{i}{2} (q_x^2 - 3q_y^2) + \frac{2\omega_{ce}}{\omega_0} q_x q_y \right) \frac{c E_0}{\omega_0 L_n(x) H} \quad (3)$$

In (2) and (3) we have assumed $q_z = 0$ implying the minimal convective losses of UH waves along the magnetic field. Treating (1) in the WKB approximation, we obtain the following dispersion relation

$$(q^2 + \chi_l(\omega_0 / 2 + i\gamma, \mathbf{q}, x))(q^2 + \chi_l(-\omega_0 / 2 + i\gamma, \mathbf{q}, x)) = \chi_{nl}(\omega_0 / 2 + i\gamma, \mathbf{q}, x) \chi_{nl}(-\omega_0 / 2 + i\gamma, \mathbf{q}, x) \quad (4)$$

Solving (4) numerically we get the dispersion curves of UH waves which are shown in Fig. 2 for $q_y \rho_e = 1.93$ (solid line) and $q_y \rho_e = 1.89$ (dashed line) and the following parameters $a = 1.1$

the pump power, $E_0(P_0, z) \propto \cos(\pi z / (2w_z))$, $k_x = \sqrt{\omega_0^2 / c^2 - \pi^2 / w_z^2}$ and ω_0 is the pump frequency. As for the experimental conditions the vacuum wavelength of microwave radiation transmitted through the waveguide $2\pi / k_x$ is much bigger than the density scale length $L_n = |\partial(n(x)/n(0)) / \partial x|^{-1}$, we ignore the spatial structure of the pump in the plasma and assume $k_x = 0$. The wavelength of a couple of electrostatic UH waves excited by the pump at half a pump wave frequency and propagating in opposite directions $\phi_1(\mathbf{r}, t) = b_1 \exp(-i\omega_0 t / 2)$,

cm, $B = 39$ mT, $n(0) = 2.2 \times 10^{10}$ cm $^{-3}$, $T_e(0) = 0.8$ eV, $v_{ea} = 4 \times 10^6$ s $^{-1}$, $P_0 = 100$ W, the parabolic density and temperature profiles. One can see the UH waves are localized in the vicinity of a local maximum of the nonlinear term in the RHS of equation (4), proportional to $\chi_{nl}(\omega_0/2, x)\chi_{nl}(-\omega_0/2, x) \propto a^2/L_n^2(x)$. The growth-rate of the TUHPD at $P_0 = 100$ W is $\gamma_{n=0} = 6 \times 10^6$ s $^{-1}$ for the fundamental mode and $\gamma_{n=4} = 5.5 \times 10^6$ s $^{-1}$ for $n = 4$. The power threshold of TUHPD predicted by theory for the above parameters is about 16 W.

4. Results and discussion

At a small plasma density no distortions of the microwave pulses in waveguide are observed (Fig. 3a). The full microwave power balance is defined as $P_0 = P_t + P_r + P_h$, where P_0 , P_t and P_r , are incident, transmitted and reflected powers, P_h is a power radiated through holes in

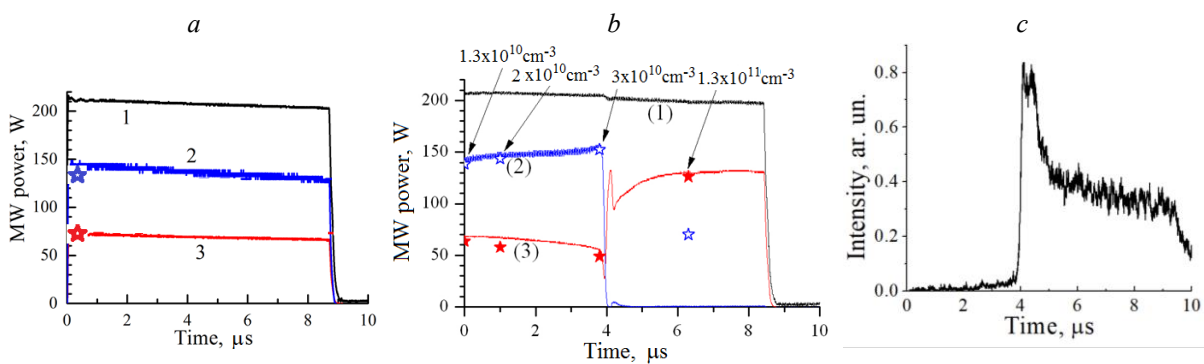


Fig. 3. Waveforms of incident (1), transmitted (2) and reflected (3) pulses at small plasma density (a) and at $n_e = 1.3 \times 10^{10}$ cm $^{-3}$ (b) and of plasma luminosity (c). Incident power $P_0 = 210$ W.

waveguide (see Fig. 1). Modelling and the measured power balance shows that power radiated through holes is about 1-2 W (about 1% of P_0). The modelling of wave transmission through the waveguide system was performed using HFSS software [5]. The simulation results are presented by stars in Fig. 3a. It should be stressed that at plasma density exceeding a threshold value after a time delay a fast decrease of both transmitted and reflected power is observed indicating the turning on of the strong anomalous absorption (see Fig. 3b). This effect is accompanied by a sharp growth of the plasma luminosity shown in Fig. 3c. The time delay of the anomalous phenomena appearance is dependent on the pump power, magnetic field and initial electron density. The threshold density needed for switching on of the anomalous phenomena is close to the theoretical UHR density dependence on the magnetic field for the half pump frequency [4] given by

$$n_e = \frac{m_e}{4\pi e^2} \left[(\pi f_0)^2 - \left(\frac{eB}{m_e c} \right)^2 \right] \quad (3)$$

The threshold power for strong absorption excitation at $B = 40$ mT and mean electron density 10^{10} cm $^{-3}$ is 20 W which is close to the theory expectations.

Based on experimental values of transmission and reflection coefficients (Fig. 3b) we can estimate the mean electron density variation during the pump pulse using it as a fitting parameter in computations using the HFSS software. Thus at the pulse beginning, the density supposed uniform in radii, is estimated as 1.3×10^{10} cm $^{-3}$. Just before the strong absorption onset, it reaches 3×10^{10} cm $^{-3}$. This slow density growth takes place probably due to the weak

collisional absorption of the pump. The collision frequency determined using [6] is $\nu = 1.4 \times 10^8 \text{ s}^{-1}$. After the anomalous absorption switch on, the estimated electron density is $1.3 \times 10^{11} \text{ cm}^{-3}$ at $t = 6 \mu\text{s}$.

Localization of the microwave absorption region in the radial plasma column direction of plasma column is determined by recording the transverse distributions of the plasma glow intensity with temporal resolution. We obtain the profile 3 (Fig. 4) with two maxima close to half radius indicating the off-axis position of the pump anomalous absorption region in rough agreement with the theory prediction.

The efficiency of the anomalous microwave power absorption is determined from the microwave power balance: $P_0 = P_t + P_r + P_h + P_{\text{abs}}$, where P_{abs} is the absorbed power. The absorption coefficient k_{abs} is given by $k_{\text{abs}} = 1 - (P_t + P_r + P_h)/P_0$. According to measurements results presented in Fig. 3, the absorption coefficient varies

drastically during the pump pulse. It is close to zero at $0 < t < 4 \mu\text{s}$ (collisional absorption), sharply reaches 80-85% at $t = 4 \mu\text{s}$ and achieve saturation at about 40-45% level at $t > 6 \mu\text{s}$.

It should be mentioned that the sharp growth of the anomalous absorption is accompanied by a burst of plasma microwave radiation registered by the heterodyne detection scheme in the half pump frequency range. The corresponding spectra measured for different times in the temporal window of $1.28 \mu\text{s}$ and averaged over 32 realisations are shown in Fig. 5. The most intensive spectrum (blue curve) is observed in the period

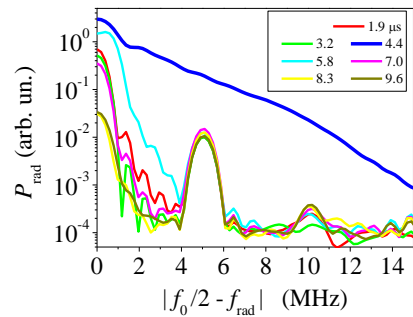


Fig. 5. Evolution of the plasma radiation spectrum in the half pump frequency range.

of the strongest suppression of the reflected signal, thus in the period of the strong anomalous absorption onset. During this period the emission is enhanced by more than two orders of magnitude.

Acknowledgements

The financial support of the RSF grant 16-12-10043 and BRFFI grant F18R-040 is acknowledged.

References

- [1] S.K. Nielsen, M. Salewski, et al., *Plasma Phys. Control. Fusion*, **55**, 115003 (2013).
- [2] E.Z. Gusakov and A.Yu. Popov, *Physics of Plasmas*, **23**, 082503 (2016)
- [3] E. Gusakov, A. Popov, P. Tretinnikov *JETP Letters* **108**, 2, (2018)
- [4] A. Altukhov, et. al., *EPJ Web of Conferences*, **157**, 03050 (2017).
- [5] <https://www.ansys.com/products/electronics/ansys-hfss>.
- [6] <https://www.bolsig.laplace.univ-tlse.fr/download>.

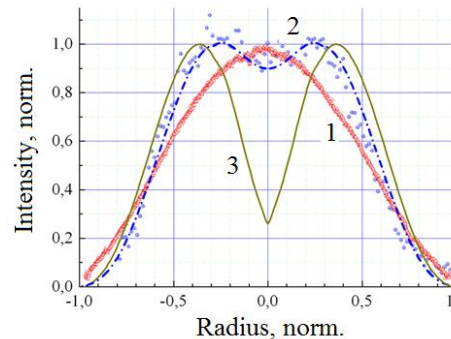


Fig. 4. Light intensity profiles.